

# Conceptual Design of a Hypervelocity Asteroid Intercept Vehicle (HAIV) Flight Validation Mission

Brent W. Barbee,<sup>\*</sup>

*NASA/GSFC, Greenbelt, MD, 20771, USA*

Bong Wie,<sup>†</sup>

*Iowa State University, Ames, IA 50011-2271, USA*

Mark Steiner,<sup>‡</sup> and Kenneth Getzandanner<sup>\*</sup>

*NASA/GSFC, Greenbelt, MD, 20771, USA*

Near-Earth Objects (NEOs) are asteroids and comets whose orbits approach or cross Earth's orbit. Very small NEOs collide with Earth regularly, and NEOs large enough to reach Earth's surface and cause damage have struck Earth in the past and will do so again. It is therefore essential that we design and test the spacecraft systems necessary to intercept and deflect or destroy incoming NEOs prior to needing to rely upon such systems during an emergency situation. Towards this end we describe current progress in a Phase 2 NASA Innovative Advanced Concepts (NIAC) research project to design a Hypervelocity Asteroid Intercept Vehicle (HAIV) and its flight validation mission. The HAIV is a two-body vehicle consisting of a leading kinetic impactor and trailing follower carrying a Nuclear Explosive Device (NED) payload. The HAIV detonates the NED inside the crater formed in the NEO's surface by the lead kinetic impactor portion of the vehicle, effecting a powerful subsurface detonation to disrupt the NEO. A simple mass proxy for the NED is carried in the HAIV for the flight validation mission. Ongoing and future research topics are discussed following the presentation of detailed flight validation mission design results produced by the NASA Goddard Space Flight Center's Mission Design Lab (MDL) in collaboration with Iowa State University's Asteroid Deflection Research Center (ADRC).

## I. Introduction

EARTH has a well-documented history of impact by asteroids and comets that were sufficiently energetic, in terms of mass and impact velocity, to cause significant damage ranging from local or regional devastation to mass extinctions. Such an asteroid or comet whose orbit approaches or crosses Earth's orbit is referred to as a near-Earth object (NEO). At present there are at least tens of thousands of undiscovered NEOs larger than 100 m in diameter, and at least hundreds of thousands of undiscovered NEOs less than 100 m in diameter. Any of these may be found to be on a collision course with Earth and therefore require a planetary defense mission to deflect or destroy it prior to Earth impact. Current NEO detection and tracking programs are making significant strides in discovering these NEOs and monitoring their orbits for future Earth impacts to provide advance warning of any threats. We have also sent a number of scientific missions to asteroids and comets that provide heritage on which future planetary defense missions can build. However, no planetary

---

<sup>\*</sup>Aerospace Engineer, Code 595, 8800 Greenbelt Road, AIAA Member.

<sup>†</sup>Vance Coffman Endowed Chair Professor, Asteroid Deflection Research Center, Department of Aerospace Engineering, 2271 Howe Hall, Room 2325, AIAA Associate Fellow.

<sup>‡</sup>Mission Design Lab Team Lead, Code 592, 8800 Greenbelt Road, AIAA Senior Member.

defense flight validation missions have been deployed and the capability to deflect or destroy a threatening NEO therefore remains unproven.

Some of the key factors in designing planetary defense systems include the size of the incoming NEO and the amount of warning time. The size of the NEO determines how much damage it would cause and places limits on our response options, while the warning time further constrains our options for dealing with the NEO. Opportunities to rendezvous with NEOs at a reasonable propellant mass cost tend to occur infrequently, so, for scenarios in which the NEO impact event is known less than 10 years in advance, the most viable option will likely be hypervelocity intercept in which our system is delivered to the NEO at high relative velocity ( $> 5$  km/s) because the propellant mass required to match the NEO's orbital velocity would be prohibitively high. Although larger NEOs are capable of causing more damage than smaller ones, the small NEOs are far more numerous and thus a small NEO impact scenario is more likely during any given time frame, all else being equal. Unfortunately, small NEOs are fainter in the night sky and therefore harder to discover and track with ground-based telescopes in advance of when they would collide with Earth. Additionally, small NEOs are more difficult for a spacecraft to target (i.e., acquire optically with onboard cameras), especially at high relative velocity. Thus the most challenging NEO mitigation scenario involves a small NEO with relatively short warning time, requiring a hypervelocity intercept for deflection or destruction of the NEO. A spacecraft system capable of reliably handling that scenario would of course be able to handle less stressing cases, i.e., more warning time, lower intercept velocities, and/or larger NEOs.

In this paper we describe research performed towards the design of such a spacecraft system by the Asteroid Deflection Research Center (ADRC) in the Department of Aerospace Engineering at Iowa State University and the Mission Design Lab (MDL) in the Integrated Design Center (IDC) at the National Aeronautics and Space Administration (NASA) Goddard Space Flight Center (GSFC). The goal of this work is to assess the technical feasibility of reliably performing hypervelocity interception of a 50 m diameter NEO and design a spacecraft and mission architecture for flight validation of the system. This research was funded by and in support of the NASA Innovative Advanced Concepts (NIAC) Phase 2 study entitled "An Innovative Solution to NASA's NEO Impact Threat Mitigation Grand Challenge and Flight Validation Mission Architecture Development."<sup>a</sup> The goals of this research project include designing a two-body Hypervelocity Asteroid Intercept Vehicle (HAIV) to deliver a kinetic impactor to the target NEO that will create a shallow crater on the NEO's surface in which the follower portion of the spacecraft will detonate a Nuclear Explosive Device (NED) immediately thereafter to effect a powerful subsurface detonation capable of disrupting the NEO; subsurface detonations are believed to be on the order of 20 times more effective at disrupting a NEO than detonations on or above the NEO's surface. The flight validation mission will carry an inert dummy payload with the same mass properties as a NED. Flight validation of this system is crucial because any NEO mitigation system must be thoroughly flight tested before it can be relied upon during a true emergency, yet no such flight validations have been performed.

## II. The Threat of NEO Impacts

Recent decades have seen considerable improvement in our understanding of the NEO population and the hazard that NEOs pose to Earth. Ground-based survey programs, such as LINEAR, the Catalina Sky Survey, and the emerging Pan-STARRS and LSST systems, have discovered many near-Earth asteroids (NEAs) and near-Earth comets (NECs). Automated computer systems, such as the Sentry system at the NASA Jet Propulsion Laboratory (JPL) and the NEODyS system at the University of Pisa, continually monitor the known NEO population to determine whether any NEOs have a non-zero probability of collision with Earth. Ground-based discovery and tracking, combined with automated impact probability monitoring, will afford us advance warning of an Earth-impacting NEO if its heliocentric orbit geometry and phasing relative to Earth allow it to be detected by ground-based telescopes prior to the time of Earth impact.

As of July 14<sup>th</sup>, 2013, 9,938 NEAs and 94 NECs have been discovered<sup>b</sup>, yielding a total of 10,032 known NEOs. 1,410 of these are classified as Potentially Hazardous Asteroids (PHAs), meaning that their Earth Minimum Orbit Intersection Distances (MOIDs) are  $\leq 0.05$  AU (approximately 7,480,000 km) and their estimated diameters are  $\geq 150$  m.

Earth is typically struck by very small NEOs (on the order of one to several meters in diameter) multiple

---

<sup>a</sup>[http://www.nasa.gov/offices/oct/early\\_stage\\_innovation/niac/2012\\_phaseII\\_fellows\\_wie.html](http://www.nasa.gov/offices/oct/early_stage_innovation/niac/2012_phaseII_fellows_wie.html), accessed 2013-07-14.

<sup>b</sup><http://neo.jpl.nasa.gov/stats/>, accessed 2013-07-14

times each year. These objects typically burn up or explode high in the upper atmosphere and thus do not generally pose a direct threat to the Earth's surface. The high altitude explosions caused by these NEOs are detectable by worldwide infrasound sensors, which allows them to be distinguished from weapons testing or deployments. Somewhat larger NEOs, up to a few tens of meters in diameter, pass within lunar distance of the Earth every few weeks. However, our telescopes do not always detect these small NEAs because their small size makes them relatively faint in the night sky. In some cases they may approach from the sunward direction and hence do not appear in our night sky at all.

Two significant NEO impact events occurred recently on February 15<sup>th</sup>, 2013. The first event of the day was the impact of an approximately 17 to 20 m NEO over the city of Chelyabinsk in Russia. The 440 kiloton explosion at an altitude of 23 km shattered many windows, damaged some buildings, and injured approximately 1500 people in the process. Only 16 hours after the Chelyabinsk event, the 40 m near-Earth asteroid (NEA) 2012 DA<sub>14</sub> reached its point of closest approach to Earth at an altitude of approximately 27,600 km. This is the closest approach on record by a NEO of that size. Despite the fact that these two events occurred only hours apart, there is no relationship between the 2012 DA<sub>14</sub> close approach and the Chelyabinsk event<sup>c</sup>.

Our planet bears the scars of past celestial bombardments, though they are largely obscured by weathering, vegetation, and the fact that the majority of Earth's surface is covered by water. Nevertheless, 184 confirmed impact structures<sup>d</sup> have been discovered on Earth thus far, many of which are larger than 20 km in diameter. Statistical models of the total NEO population allow us to estimate how many NEOs remain to be discovered, and recent data from the NEOWISE mission has yielded an updated estimate of the size of the NEO population. The estimated population of NEOs > 1 km in diameter is nearly 1000; just over 90% of these have been discovered and determined to not pose a threat to Earth. However, there are an estimated 16,300 NEOs with diameters between 100 and 1000 m yet to be discovered. Thus far approximately 3,000 NEOs with diameters < 100 m have been discovered and there may well be hundreds of thousands, if not millions, of NEOs in this size category yet to be discovered. Thus there are many thousands of undiscovered NEOs lurking in our inner solar system large enough to cause significant damage, and we must be prepared to deflect or destroy any that are found to be on a collision course with our planet.

### III. Space Flight Heritage Relevant to Planetary Defense

Thus far there have been no flight missions to validate planetary defense techniques or technologies. However, between 1986 and 2011, a total of 11 science spacecraft have performed flybys of 6 comets and 7 asteroids, and rendezvoused with 3 asteroids. The first of these were the Vega 1, Vega 2, and Giotto spacecraft, all of which performed flybys of comet 1P/Halley in 1986. The Galileo spacecraft closely approached two asteroids: 951 Gaspra in 1991 and 243 Ida in 1993. Meanwhile, Giotto performed a flyby of comet 26P/Grigg-Skjellerup in 1992. In 1997, the NEAR-Shoemaker spacecraft flew past the asteroid 253 Mathilde on the way to the asteroid 433 Eros, where the spacecraft entered a captured orbit and performed an extended scientific survey. During the same time frame, the Deep Space 1 spacecraft performed a flyby of asteroid 9969 Braille in 1999 and comet 19P/Borrelly in 2001. Following this, the Stardust spacecraft flew by asteroid 5535 Annefrank in 2002 and comet 81P/Wild in 2004. With the exception of NEAR-Shoemaker, all of these missions only flew past the asteroids or comets at distances of several hundred to several thousand kilometers.

This changed in 2005 when the Deep Impact spacecraft successfully deployed an impactor to collide with comet 9P/Tempel. During the same year, the Hayabusa/MUSES-C spacecraft rendezvoused with asteroid 25143 Itokawa and eventually returned tiny grains of asteroid material to Earth. The Rosetta spacecraft flew past the asteroids 2867 Steins in 2008 and 21 Lutetia in 2010 on its way to a 2014 rendezvous with comet 67P/Churyumov-Gerasimenko. After flying past comet 9P/Tempel in 2005, The Deep Impact spacecraft continued operating in an extended mission and was directed to perform a flyby of comet 103P/Hartley in 2010. Deep Impact may be re-tasked yet again to perform a flyby of a PHA known as 2002 GT during the year 2020. In 2011, the Stardust spacecraft performed a flyby of the Deep Impact target (9P/Tempel) and was able to collect images of the impact site.

The Dawn mission is currently in orbit around 4 Vesta, the largest known main belt asteroid (now understood to be a proto-planet thanks to data collected by Dawn), and will proceed to rendezvous with the dwarf

<sup>c</sup>[http://neo.jpl.nasa.gov/news/fireball\\_130301.html](http://neo.jpl.nasa.gov/news/fireball_130301.html), accessed 2013-07-14

<sup>d</sup><http://www.passc.net/EarthImpactDatabase/index.html>, accessed 2013-07-14

planet Ceres, also located in the main asteroid belt, during the year 2015. NASA is currently developing the Origins Spectral Interpretation Resource Identification Security-Regolith Explorer (OSIRIS-REx) mission, which will launch in the year 2016 to rendezvous with the PHA known as 101955 Bennu (1999 RQ<sub>36</sub>) and return to Earth with samples of the asteroid in 2023. The Japanese space program is currently considering an asteroid sample return mission known as Hayabusa 2, which would launch in 2014 with the goal of returning samples from the PHA known as 162173 (1999 JU<sub>3</sub>), and a mission named Hayabusa Mk2 to the dormant comet designated 4015 Wilson-Harrington (1979 VA). Finally, the European Space Agency (ESA) is currently studying the MarcoPolo-R mission concept, in which samples would be returned from the PHA designated 34184 (2008 EV<sub>5</sub>). This mission was originally targeting the binary asteroid 175706 (1996 FG<sub>3</sub>).

Each of the aforementioned science missions required at least several years, in some cases 5 to 6 years or more, for mission concept development and spacecraft construction prior to launch. It is also important to note that some of these missions were originally targeting different asteroids or comets than those that were actually visited. This is because the mission development schedules slipped and launch windows for particular asteroids or comets were therefore missed. Additionally, several of these missions experienced hardware or software failures or glitches that compromised the completion of mission objectives. None of those things would be tolerable for a planetary defense mission aimed at deflecting or destroying an incoming NEO. Thus, while the impressive scientific missions that have been sent to asteroids and comets so far have certainly provided future planetary defense missions with good heritage on which to build, we are clearly not ready to respond reliably to a threatening NEO scenario.

It is also important to note that most of the flyby missions visited asteroids or comets that range in size from several kilometers to several tens of kilometers, and the flyby distances ranged from several tens of kilometers to several thousand kilometers. The sole exception to this is the Deep Impact mission, which succeeded in delivering an impactor to the target. However, the mission was aided by the fact that comet 9P/Tempel, is  $7.6 \times 4.9$  km in size and therefore provided a relatively large target to track and intercept. Consequently, the Deep Impact mission was not intended to be a planetary defense technology flight validation mission. For planetary defense missions requiring NEO intercept, the requirements will be far more stringent: NEO targets with diameters as small as 50 m will have to be reliably tracked and intercepted at hypervelocity (5–30 km/s), with impact occurring within mere meters of the targeted point on the NEO's surface. This will require significant evolution of the autonomous Guidance, Navigation, and Control (GNC) technology currently available for spacecraft missions to NEOs. Furthermore, none of the potential planetary defense mission payloads to deflect or destroy a NEO have ever been tested on NEOs in the space environment. Significant work is therefore required to appropriately characterize the capabilities of those payloads, particularly the ways in which they physically couple with a NEO to transfer energy or alter momentum, and ensure robust operations during an actual emergency scenario.

When a hazardous NEO on a collision course with Earth is discovered we will not have the luxury of selecting a target NEO suitable for our mission design purposes or changing our choice of target if our development schedule slips. Instead, nature will have selected the target for us, along with whatever challenges are posed by its orbit and physical characteristics. Making preparations now is essential because we will only have one chance to deploy an effective and reliable defense.

## IV. Overview of the HAIV Mission Concept

The HAIV system and mission architecture were initially developed during a NIAC Phase 1 research study<sup>1</sup> and preliminary results prior to the conclusion of that study have also been documented in the technical literature.<sup>2,3</sup> The HAIV concept combines a kinetic impactor with a NED payload carrier to execute a subsurface detonation with the goal of disrupting the target NEO. A notional depiction of the HAIV system closing in on a target NEO is shown in Figure 1. While standalone kinetic impactors have been proposed and studied for the purpose of deflecting (rather than disrupting) a NEO, the purpose of the kinetic impactor portion of the HAIV is to create a shallow crater in the surface of the target NEO. The NED carrier portion of the HAIV, which is following immediately behind the leading kinetic impactor portion, flies into the crater and detonates the NED before striking the bottom of the crater. The lead kinetic impactor portion of the HAIV and the follower portion housing the NED separate before impacting the NEO, and the method of separation (e.g., free-flying, connected by a boom, etc.) is still under consideration. Figure 2 provides a high-level graphical summary of the process.

The result is a slightly subsurface nuclear detonation that is approximately 20 times more effective at



Figure 1. HAIV spacecraft closing in on target NEO.

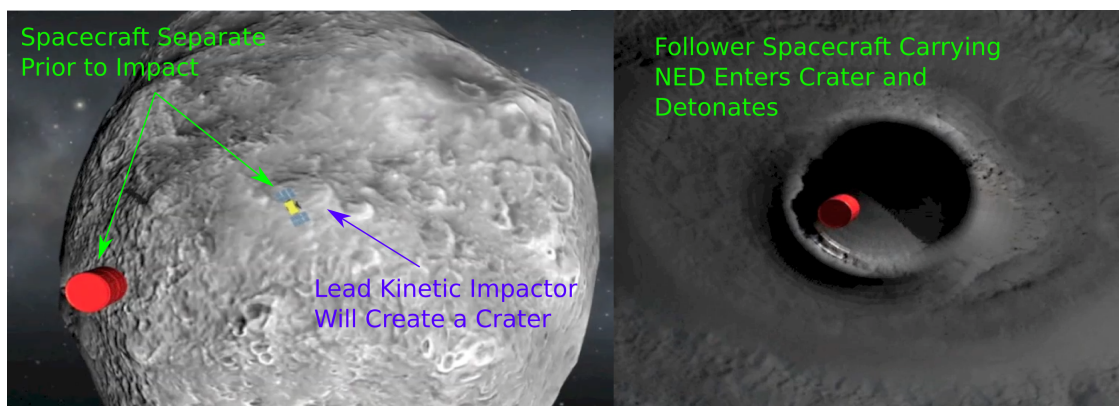


Figure 2. Separated HAIV system creates crater on NEO and detonates NED within.

disrupting the target NEO than a surface or standoff detonation. Figure 3 shows simplified 2-D computational modeling and simulation of a penetrated, 70 kiloton nuclear explosion for a 70 m asymmetric reference target body.<sup>1,3</sup>

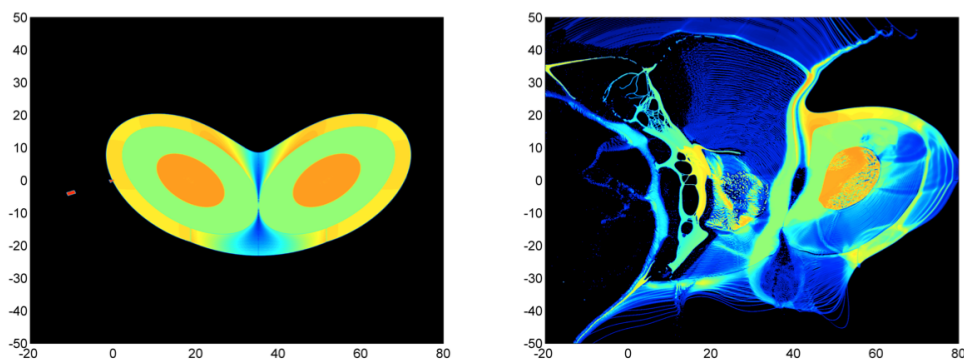


Figure 3. Simulated disruption of a small asymmetrically shaped NEO by a subsurface NED detonation.

The enhanced effectiveness of the subsurface detonation reduces the yield (mass) of the NED required to deal with a given NEO, all else being equal, and that improves responsiveness by not over-burdening the launch vehicle. Responsiveness is important because one of the primary objectives of the HAIV design is to

provide a reliable solution for dealing with short warning time ( $< 10$  years of warning) scenarios. In such scenarios the HAIV will need to be launched onto a direct high-energy trajectory to intercept the NEO not long before the NEO would have struck the Earth absent our intervention. It is a consequence of orbital dynamics that such intercept trajectories tend to have high relative velocities, in the hypervelocity regime (e.g., 5–30 km/s), between the HAIV and NEO at the time of intercept. A prohibitively large mass of propellant would be required to nullify that relative velocity for rendezvous with the NEO, which motivates the design of a robust hypervelocity intercept platform. Furthermore, we exploit the hypervelocity nature of the intercept by using the leading kinetic impactor portion of the HAIV to create the shallow crater for the subsequent subsurface NED detonation. The primary challenges include developing robust and precise GNC systems capable of reliably performing hypervelocity intercept of NEOs and creating highly responsive, accurate, and reliable hypervelocity impact detection and NED detonation systems.

## V. Notional Flight Validation Mission Target Selection

The ADRC has been developing trajectory scan techniques for identifying the best NEO targets for various flight validation mission concepts.<sup>4,5,6</sup> Those techniques were further developed to perform trajectory scans for thousands of NEOs to identify the best choice of target NEO for the notional flight validation mission scenario that we would then study in the MDL. One of our primary criteria for the mission is safety—we do not want the flight validation mission to pose any risk of turning a harmless NEO into an Earth impactor. For that reason we restrict our candidate target set to only include NEOs from the Amor and Atira groups, whose orbits are entirely exterior or interior to Earth’s orbit, respectively.<sup>e</sup>

Our ultimate goal is to develop a robust capability to perform hypervelocity intercept of NEOs as small as 50 m in size, but we decided that a somewhat larger target would be more appropriate for the very first flight validation mission. Figure 4 depicts the trade space that we considered. As indicated in Figure 4, we

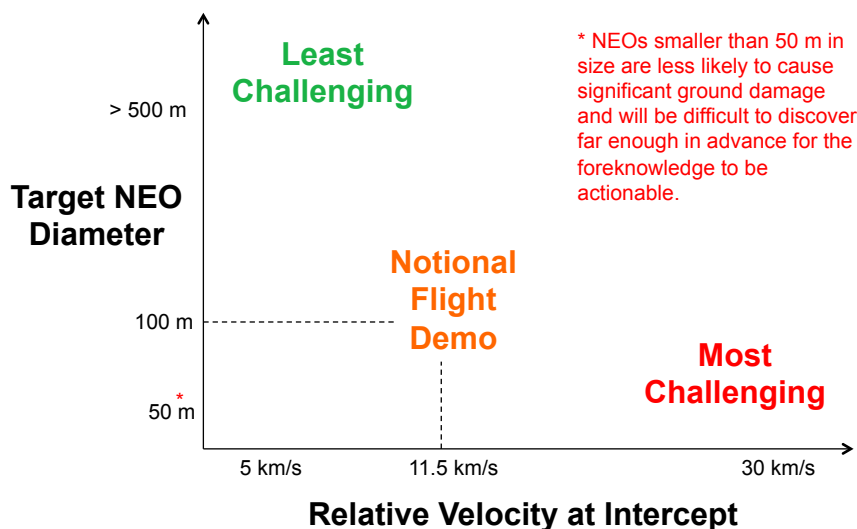


Figure 4. Depiction of the trade space for selecting a target NEO for a flight validation mission.

decided that intercepting an approximately 100 m size NEO at 11.5 km/s provides a practical scenario for the very first flight validation mission, sufficiently challenging to test the capability we want to prove, but not so challenging as to be unreasonable for the first effort. We therefore filtered our list of candidate targets to identify those with estimated diameters around 100 m.

Another consideration in our target search is how well the orbit of the NEO is known. If there is too much uncertainty in our knowledge of the NEO’s orbit it may not be possible to guide the HAIV to a precision intercept with the NEO. The quality of NEO orbit knowledge is usually expressed by the Orbit Condition Code (OCC)<sup>f</sup>, which is an integer scale describing the amount of along-track uncertainty in the NEO orbit

<sup>e</sup><http://neo.jpl.nasa.gov/neo/groups.html>, accessed 2013-07-15.

<sup>f</sup>OCC is also known as the Minor Planet Center (MPC) “U” parameter, for which the technical details are provided at <http://www.minorplanetcenter.net/iau/info/UValue.html>, accessed 2013-07-15.

knowledge. The size, shape, and orientation of NEO orbits are generally easier to estimate than the position of the NEO along its orbital path, and the location of the NEO on its orbit is therefore usually the least well known aspect of the NEO's orbit. The OCC scale ranges from 0 (a very well known orbit) to 9 (very poor orbit knowledge), and NEOs with  $OCC > 5$  are generally considered “lost” for the purposes of locating them in the sky during future observing opportunities. We thus applied a filter of  $OCC \leq 5$  to our NEO target search.

In summary, our trajectory scans were applied to Amor and Atira NEOs with estimated diameter near 100 m and  $OCC \leq 5$ . The trajectory scan constraints included Earth departure characteristic energy  $C_3 \leq 12.5 \text{ km}^2/\text{s}^2$ , Earth departure date between 2018 and 2020, Sun-Spacecraft-Earth (SSE) angle at the time of intercept  $> 3^\circ$ , and phase angle at intercept  $\leq 90^\circ$ . The SSE angle is measured between the vector that points from the spacecraft to the Sun and the vector that points from the spacecraft to the Earth. If the SSE angle is too small then the Sun may interfere with communications between the spacecraft and Earth, and we require a good communications link with the spacecraft, especially at the time of NEO intercept, in order to collect the telemetry needed to confirm the success of the experiment. The phase angle at intercept is measured between the velocity vector of the spacecraft relative to the NEO and the heliocentric position vector of the NEO at the time of intercept. A phase angle of zero places the spacecraft directly between the Sun and the NEO at the time of intercept, while a phase angle of  $90^\circ$  means that the spacecraft approaches the NEO orthogonal to the NEO-Sun line. Designing the trajectory so that a small value of the phase angle obtains provides a situation in which the Sun is naturally illuminating the full face of the NEO, or nearly so, from the spacecraft's perspective during terminal approach, which is highly advantageous for optical acquisition of the NEO with the spacecraft's onboard cameras and especially important for small NEOs that are optically faint even under such ideal circumstances.

After analyzing the trajectory scan results we settled on the NEA designated 2006 CL<sub>9</sub> as the notional target for our conceptual flight validation mission. The physical and orbit properties<sup>g</sup> of 2006 CL<sub>9</sub> are presented in Table 1. The orbital elements for the NEA presented in Table 1 are heliocentric ecliptic J2000 osculating orbital elements at epoch JD 2456400.5 (2013-04-18.0) Temps Dynamiques Barycentrique, Barycentric Dynamical Time (TDB) (JPL Orbit ID 26).

**Table 1. Physical and orbital properties of notional flight validation mission target 2006 CL<sub>9</sub>.**

Property	Value
Absolute magnitude, $H$	22.73
Estimated diameter w/ $p = 0.13$	104 m
Estimated diameter w/ $p = 0.25$	75 m
Rotation period (hours)	$0.145 \pm 30\%$
Semi-major axis, $a$ (AU)	1.34616
Eccentricity, $e$	0.23675
Inclination, $i$	$2.93551^\circ$
Longitude of Ascending Node, $\Omega$	$139.313^\circ$
Argument of Perihelion, $\omega$	$9.94912^\circ$
Mean Anomaly at Epoch, $M$	$209.664^\circ$
OCC	5
Earth MOID (AU)	0.03978

Another factor in our selection of 2006 CL<sub>9</sub> is that while its OCC of 5 would present navigation challenges for our mission, there may be opportunities to gather more ground-based observations of this NEA within the next couple of years, which may improve our knowledge of its orbit and thus reduce the OCC. It happens that this NEA meets the criteria for NASA's Near-Earth Object Human Space Flight Accessible Targets Study (NHATS)<sup>h</sup> <sup>7</sup> and the next upcoming observing opportunity is among the NHATS data published for the NEA<sup>i</sup>. These data show that the NEA should be optically observable from Earth again in June of 2014

<sup>g</sup><http://ssd.jpl.nasa.gov/sbdb.cgi?sstr=2006CL9>, accessed 2013-07-15.

<sup>h</sup><http://neo.jpl.nasa.gov/nhats/>, accessed 2013-07-15.

<sup>i</sup><http://neo.jpl.nasa.gov/cgi-bin/nhats?sstr=2006CL9&dv=12&dur=450&stay=8&launch=2015-2040>, accessed 2013-07-15.

with a peak visual magnitude of 22.9.

Note that two estimated diameter values for 2006 CL<sub>9</sub> are presented in Table 1 based on the parameter  $p$ , which is the geometric albedo of the NEA (a measure of how optically reflective its surface is). The albedos of NEOs vary widely and are very difficult to ascertain from ground-based observations. This leads to significant uncertainty in the physical size of most known NEOs. The problem can be summarized thusly: small shiny objects can have the same brightness in the sky as large dull objects. The brightness of a NEO, expressed by absolute magnitude,  $H$ , is much better constrained (because it is directly observed) than albedo. We must assume an albedo for our NEA in order to compute the estimated diameter<sup>j</sup> and as shown in Table 1 we used albedo values of 0.13 and 0.25. Those are reasonable values for NEA albedo and yield an estimated size between 75 and 105 m, which is near the 100 m value we desire. All that being said, note that the NHATS data for this NEA show an estimated diameter range of 49 to 221 m, based on albedos of 0.6 and 0.03, respectively, and so it is possible that this NEA is anywhere from half the size to double the size we have estimated with an albedo of 0.13.

The mission trajectory selected for 2006 CL<sub>9</sub> is summarized in Table 2. The baseline trajectory design is based on patched conics with Lambert targeting applied to high-fidelity ephemerides for the Earth and NEA, and therefore no deterministic  $\Delta v$  is required on the part of the spacecraft in this initial trajectory design. However, statistical trajectory course corrections were computed during the MDL study and are elaborated on in a subsequent section.

**Table 2. Notional flight validation mission trajectory selected for 2006 CL<sub>9</sub>.**

Property	Value
Earth departure date	2019-08-02
Earth departure $C_3$	11.99 km <sup>2</sup> /s <sup>2</sup>
Flight time to intercept NEO	121.41 days
Relative velocity at intercept	11.5 km/s
Approach phase angle	3.04°
Max. distance from Earth	0.36 AU
Max. distance from Sun	1.28 AU

## VI. Mission Design Lab Results

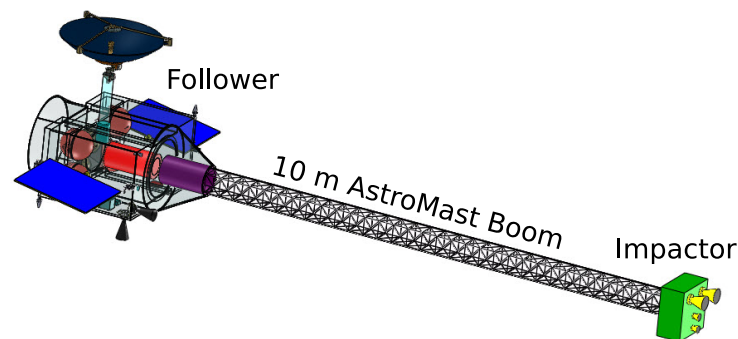
The primary objective of the MDL study was to assess the technical feasibility of deploying a spacecraft to intercept a small (50–100 m) NEO within 10 m of its center with  $3\sigma$  confidence at high relative velocity ( $> 10$  km/s) in order to provide a viable planetary defense solution for short warning time scenarios. The MDL performed this assessment by developing a preliminary spacecraft systems concept for the HAIV capable of reliably delivering a notional NED payload to a target NEO and transmitting adequate telemetry for validation of system performance. In addition to the conceptual spacecraft design, the MDL created associated plans for the supporting mission and ground operations in order to provide an overall mission architecture. The MDL worked to design a fully capable HAIV (rather than a simplified test platform) and apply the fully capable design to a suitable practice target NEO (as described previously in the section about target selection). The MDL endeavored to make the flight validation mission affordable through judicious mission design rather than via a scaled-down less expensive flight demonstration platform.

The primary design drivers are the high relative velocity at impact and the precision timing required for detonation of the NED in the shallow crater excavated by the leading kinetic impactor portion of the vehicle. The MDL carefully considered what systems equipment should be placed on the lead portion (kinetic impactor) of the HAIV and what should be placed on the follower portion (NED payload carrier). Additionally, high reliability is required because there will only be one opportunity to successfully strike the target NEO. These considerations make it clear that the HAIV will need to be a highly responsive system with onboard autonomous control because of the latency inherent in ground commanding and the highly dynamic environment of the terminal approach phase. Yet another challenging aspect of this mission is that

<sup>j</sup><http://www.physics.sfasu.edu/astro/asteroids/sizemagnitude.html>, accessed 2013-07-15.



The overall mechanical design for the HAIV created by the MDL is presented in Figure 5 and shows the leading impactor portion of the vehicle, the trailing follower portion of the vehicle (carrying the dummy mass proxy for the NED), and the 10 m AstroMast extendable boom that provides the necessary separation between the impactor and follower during NEO impact while ensuring that the two parts of the vehicle remain collinear during impact. The length of the boom is customized for the particular mission scenario at hand such that the boom length provides an appropriate delay time between when the impactor creates the crater on the NEO and when the follower arrives in the crater and detonates the NED. The appropriate delay time is of course dependent on the terminal approach profile, which is chiefly dominated by the HAIV velocity relative to the NEO at impact. Figure 6 shows another view of the HAIV with selected dimensions and mass properties labeled, while Figure 7 provides a more detailed view of the follower portion of the HAIV with selected subsystem components labeled.

[illegible]

In the following we present a mission overview, detailed descriptions of selected subsystems, the mission cost estimate, and a discussion of key future research topics identified during the MDL study.

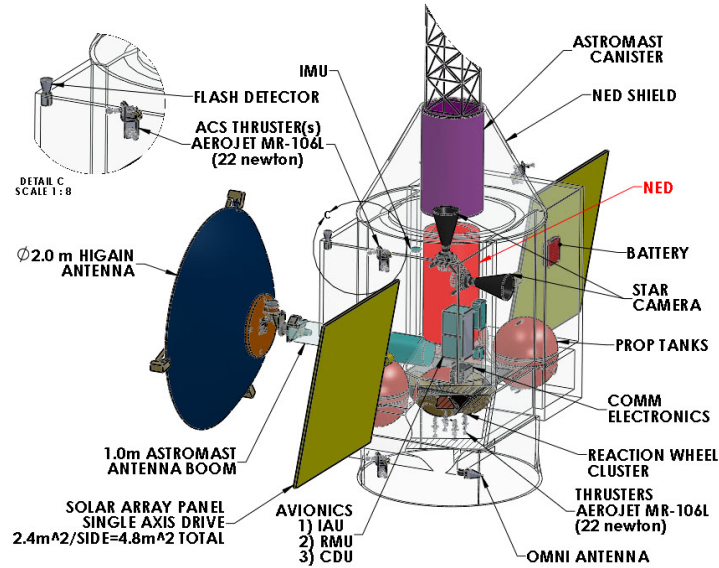


Figure 7. Detail view of the follower portion of the HAIV showing selected subsystem components.

## VI.A. Mission Overview

For launch vehicles, the MDL considered the United Launch Alliance (ULA) Atlas V 400/500 Evolved Expendable Launch Vehicle (EELV) Series, the SpaceX Falcon 9, and the Boeing Delta IV series. All of these launch vehicles provide sufficient mass capability at the desired Earth departure  $C_3$  but the Atlas V is the only EELV currently covered under the NASA Launch Services Program II contract. As such, the Atlas V 401 with a 4 m fairing was selected as the primary launch vehicle for the MDL study. The HAIV launch configuration in the Atlas V 401 payload fairing is shown in Figure 8. Accordingly, the HAIV will launch from Cape Canaveral Air Force Station (CCAFS).

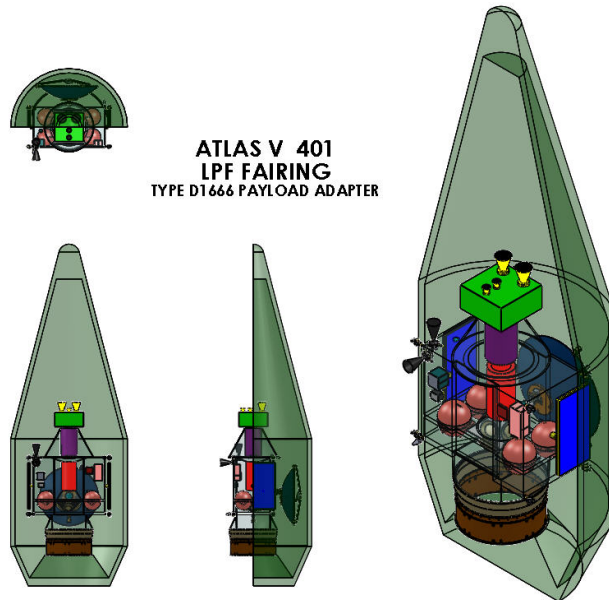


Figure 8. HAIV launch configuration.

Figure 9(a) presents the overall mission timeline, beginning with launch on August 2<sup>nd</sup>, 2019. Launch is followed by two weeks of on-orbit checkout (during the Earth departure trajectory), which leads into approximately 121 days of outbound cruise towards the target NEO. Although the flight validation mission

only carries a simple mass proxy for the NED, we will treat it as if it were a live explosive payload and go through the same steps that we would with the live payload. Thus the payload is “armed” 30 days prior to NEO impact (I - 30 days). The onboard targeting system is engaged at I - 48 hours and images of the NEO (still very small in the camera Field Of View (FOV)) begin to be transmitted to the ground. The boom is then extended to deploy the impactor at I - 24 hours.

Figure 9(b) shows the mission timeline for the final 2 hours. At I - 2 hours the ground relinquishes control to the vehicle and the Terminal Guidance Maneuvers (TGMs) begin. At the final 60 seconds before impact the HAIV is 660 km away from the NEO and is transmitting 10 images per second to the ground, with the final image downlinked at I - 1 second. At I - 0 the impactor contacts the surface of the NEO (creating a shallow crater) and that event causes the fire command to be issued to the NED mass proxy (which is instrumented with the same circuitry that would be used with an actual NED). At I + 1 millisecond the follower portion of the vehicle enters the crater and the NED would detonate at this time (due to the fire command having been issued at the proper time 1 millisecond prior to crater entry).

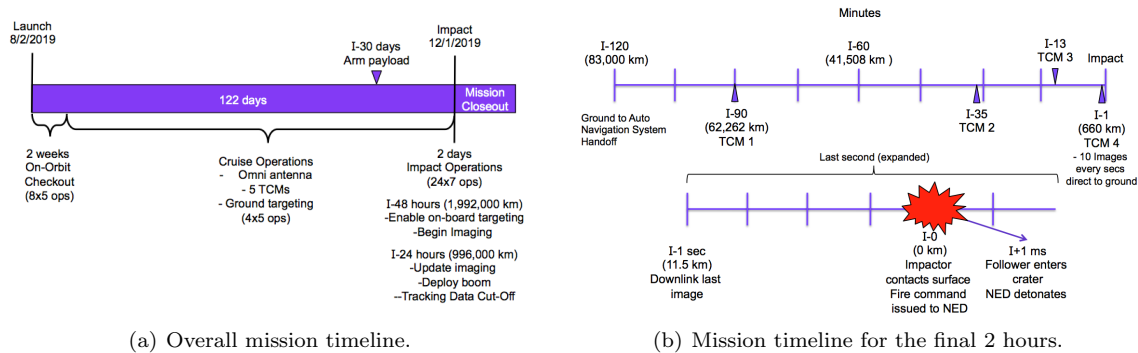


Figure 9. HAIV flight validation mission timeline.

Table 3 summarizes the performance of the instruments assumed for the HAIV. The NAVCAM provides images centered on the NEO (which only occupies a very small percentage of the FOV until shortly before impact, as will be shown in a subsequent section). These images are used for internal navigation functions onboard the spacecraft and are also transmitted to the ground to provide situational awareness, enable reconstruction of the spacecraft’s final approach to impact, and provide pre-impact visible wavelength images of the impact site. The IMPACTCAM collects and transmits imagery of the NEO at a higher frame rate and lower resolution during the final 60 seconds before impact to provide additional situational awareness and facilitate an in-depth reconstruction of the spacecraft’s collision with the NEO so that the ground can verify that impact accuracy requirements were met correctly in post-processing. More details about these instruments are provided in subsequent sections. Finally, a hypervelocity contact sensor is utilized to detect the collision of the leading kinetic impactor portion of the vehicle with the NEO, and that collision detection signal is used to send the fire command to the NED proxy payload. Note that communications between the impactor and follower portions of the vehicle are hard-wired (i.e., no radio signals are exchanged between the vehicles).

Table 3. Instrument performance values.

Instrument	Data Rate	Frame Rate	Start Time
NAVCAM (Internal Navigation Frames)	8.4 Mbps	1/min	I - 48 hours
NAVCAM (Image Frames for Transmission to Ground)	400 kbps	5/sec	I - 48 hours
IMPACTCAM	65 kbps	10-17/sec	I - 60 seconds
Contact Sensor	-	-	Triggered by Impact

The detailed mass summary for the HAIV is provided in Table 4 according to the two parts of the HAIV (impactor and follower), their subsystems, and the NED proxy payload. The vehicle design includes the necessary redundancy for a Class A mission, and this is reflected in the mass values shown. The total wet

mass of the HAIV launch is computed to be about 1200 kg, including contingencies. However, the Atlas V 401 has approximately twice that mass capability at our Earth departure  $C_3$  of  $12 \text{ km}^2/\text{s}^2$ . That provides a substantial amount of margin for spacecraft mass growth during development leading up to launch. It also means that a smaller (less expensive) launch vehicle could theoretically be utilized for this mission if such a launch vehicle existed. It is important to note that the total propellant mass required for the mission is only 64 kg. The mission  $\Delta v$  and propulsion system design are detailed in subsequent sections, and those discussions show that the total propellant capacity of the HAIV is about 364 kg. Thus, if the propellant tanks are filled to capacity then the propellant load becomes 363.8 kg. That raises the Current Best Estimate (CBE) spacecraft wet mass (launch mass) to 1345 kg (from 1045 kg in Table 4), and with a contingency of 12% the Maximum Expected Value (MEV) spacecraft wet mass (launch mass) becomes 1500.7 kg. That leaves a launch vehicle throw mass margin of 814 kg (down from 1114 kg in Table 4) or 54.3% (down from 92.8%). The mass margin above 15% becomes 39.3% (down from 77.8%). It is therefore possible to provide the spacecraft with a significant amount of excess  $\Delta v$  capability while maintaining very robust mass margins.

## VI.B. Flight Dynamics

As described previously, the launch vehicle selected by the MDL for the conceptual flight validation mission is the Atlas V 401. The  $3\sigma$  dispersion on the Earth departure  $C_3$  is  $0.15 \text{ km}^2/\text{s}^2$ , which leads to a  $\Delta v$  for launch dispersion correction of approximately 26 m/s, including maneuver execution errors. The Declination of the Launch Asymptote (DLA) and Right ascension of the Launch Asymptote (RLA) are  $52.4^\circ$  and  $-12^\circ$ , respectively. The time of injection into the outbound Earth departure hyperbola is 2019-08-02, 08:47:26.443 UTC. The flight time to NEO intercept is 121.41 days, which leads to a time of intercept of 2019-12-01, 18:37:50.443 UTC. The velocity relative to the target at intercept is 11.5 km/s and the approach phase angle is  $3^\circ$ . The maximum distance from the Earth is 0.36 AU and the maximum distance from the Sun is 1.28 AU. This particular trajectory design was assumed to be the middle of the launch window. The conditions associated with the opening and closing of the mission launch window were computed and are summarized in Table 5. The baseline trajectory solution for the middle of the launch window is plotted in Figure 10.

The total post-launch  $\Delta v$  budget for the mission is 37.1 m/s, detailed in Table 6. In Table 6 TCM stands for Trajectory Correction Maneuver, TGM stands for Terminal Guidance Maneuver, L stands for Launch, and I stands for Impact. The development of the TGM portion of the budget is based on specialized terminal guidance analysis that is presented subsequently.

## VI.C. Navigation and Terminal Guidance

The MDL performed a complete navigation simulation of the terminal approach phase beginning at I - 2 hours. The navigation simulation included a linear covariance analysis and a Monte Carlo error analysis. The navigation simulation utilized a sequential Kalman filter with observations derived from the asteroid centroid location in the sensor CCD (Charge-Coupled Device). The navigation filter is solving for the inertial position and velocity of the spacecraft with respect to the asteroid. The simulation software utilized is the Orbit Determination Toolbox (ODTBX)<sup>k</sup>.

The optical navigation sensors modeled in the simulations are based on the Deep Impact mission's Impactor Targeting Sensor (ITS), which has a FOV of  $0.6^\circ$ , a focal length of 2101 mm, and a resolution of  $1024 \times 1024$ . The navigation relies on identification of the target body centroid in the sensor field of view. The acquisition requirement is to be able to detect a 13<sup>th</sup> apparent magnitude object with a signal-to-noise ratio of at least 10 within a 5 second exposure.

Figure 11(a) shows when the ITS is able to acquire the target NEO in terms of time until impact for the high (0.25) and low (0.13) albedo cases defined for this study. The effect of NEO albedo is quite clear: acquisition occurs at I - 35.65 hours for the high albedo case and only I - 17.68 hours for the low albedo case. If the NEO's albedo turns out to be  $< 0.13$ , it could be problematic for the terminal guidance sequence due to acquisition occurring too late prior to impact. This problem is being studied further in ongoing research. Figure 11(b) shows the size of the NEO in the ITS FOV as a function time before impact. The high intercept

<sup>k</sup>ODTBX is an advanced mission simulation and analysis tool used for concept exploration, proposals, early design phases, and rapid design center environments. ODTBX is developed by the Navigation and Mission Design Branch at NASA Goddard Space Flight Center. The software is released publicly under the NASA Open Source Agreement and is available on SourceForge at <http://sourceforge.net/projects/odtbx/>, accessed 2013-07-15.

**Table 4. Spacecraft mass summary with minimum propellant load.**

Payload Mass			
NED	CBE (kg)	Contingency (%)	MEV (kg)
Payload Dry Mass	300.0	0	300.0
Payload Wet Mass	0.0	0	0.0
Total Payload Mass	300.0	0	300.0
Impactor Bus Dry Mass			
	CBE (kg)	Contingency (%)	MEV (kg)
ACS-NAVCAM 1,2 ( $\times 2$ )	10.0	0	10.0
ACS-IMPACTCAM 1,2 ( $\times 2$ )	2.0	0	2.0
ACS-Impact Sensor	2.0	0	2.0
Mechanical Impactor	136.0	0	136.0
Power (2 Lithium-Ion Batteries, 12.33 kg)	12.3	0	12.3
Spacecraft Bus Dry Mass total	162.3	0	162.3
Follower Bus Dry Mass			
	CBE (kg)	Contingency (%)	MEV (kg)
Attitude Determination and Control	52.7	30	68.4
Mechanical	82.5	30	106.7
AstroMast Boom	38.3	30	49.7
Thermal	32.8	30	42.6
Propulsion	80.3	30	104.4
Power (SA, Battery, Harness, no PSE)	92.9	30	120.7
Avionics	59.2	30	77.0
Communications	80.8	30	105.0
Spacecraft Bus Dry Mass Total	681.2	23	836.8
Total Spacecraft Mass			
	CBE (kg)	Contingency (%)	MEV (kg)
Payload Total	300.0	0	300.0
Spacecraft Bus Dry Mass	681.2	23	836.9
Total Dry Mass	981.2	16	1136.9
Propellant (Hydrazine + Pressurant)	64.0	0	64.0
Spacecraft Wet Mass (Launch Mass)	1045.2	15	1200.9
Launch Vehicle Evaluation			
Launch Vehicle Capability (Atlas V 401) (kg)			2315
Launch Vehicle Throw Mass Margin (kg)			1114
Launch Vehicle Throw Mass Margin (%)			92.8
Margin Above 15%			77.8

velocity and the NEO's small size mean that the NEO will not even begin to fill the FOV until a few seconds before impact.

The error sources modeled in the navigation simulation include spacecraft a priori state uncertainties of 5 km in position and 1 cm/s in velocity, 3-axis spacecraft attitude uncertainty of 10  $\mu$ rad, random centroid pixel noise of 0.05 pixels with a 0.1 pixel bias, and proportional and fixed maneuver execution errors of 1%

Table 5. Preliminary launch window.

	Open	Middle	Close
Launch date	2019-07-21	2019-08-02	2019-08-12
Earth departure $C_3$ (km <sup>2</sup> /s <sup>2</sup> )	22.48	11.99	8.44
RLA	58.6°	52.4°	38.9°
DLA	−3.1°	−12.0°	−20.8°
Relative velocity at intercept (km/s)	13.4	11.5	10.0

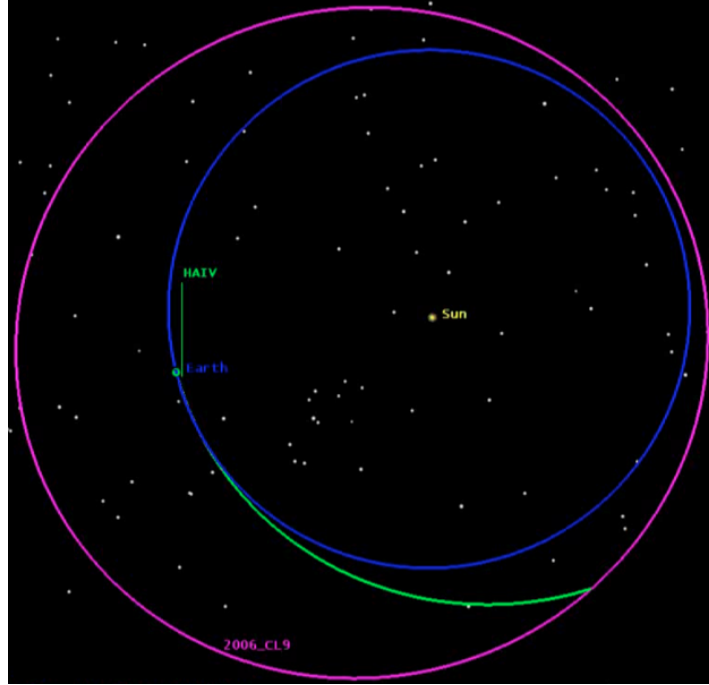
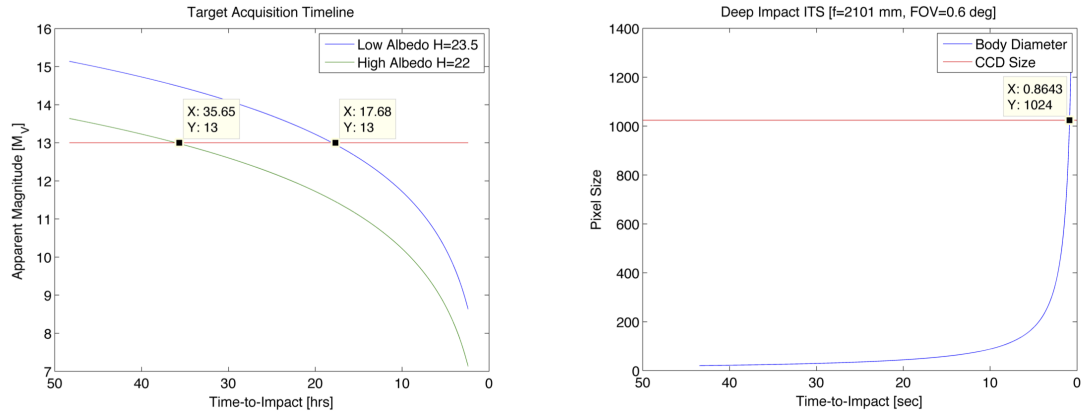


Figure 10. Ecliptic plane projection of the Earth's orbit (blue), the orbit of 2006 CL<sub>9</sub> (violet), and the HAIV intercept trajectory (green).

Table 6. Maneuver schedule and  $\Delta v$  budget.

Maneuver	$\Delta v$ (m/s)	Time	Correction	$\Delta v$ Error (%)	$\Delta v$ Error (m/s)
TCM 1	26.0	L + 01 days	Launch vehicle insertion ( $3\sigma$ )	10	2.6
TCM 2	2.8	L + 10 days	TCM 1 error	5	0.140
TCM 3	0.3	L + 30 days	TCM 2 error	5	0.015
TCM 4	0.2	L + 60 days	TCM 3 error	5	0.010
TCM 5	0.3	L + 90 days	TCM 4 error	0	0.000
TGM 1	3.1	I - 90 min	Nav and TCM 5 error	-	-
TGM 2	0.4	I - 35 min	Nav and TGM 1 error	-	-
TGM 3	0.5	I - 13 min	Nav and TGM 2 error	-	-
TGM 4	3.5	I - 60 secs	Nav and TGM 3 error	-	-
Total $\Delta v$	37.1				



(a) Optical acquisition time for low and high NEO albedo. (b) NEO size in ITS FOV as a function of time.

Figure 11. Timelines for NEO acquisition and size in ITS FOV.

and 1 mm/s, respectively. All of these error values are  $1\sigma$ .

Figure 12 presents a block diagram for the Autonomous Navigation System (ANS) that is modeled in simulation to perform navigation and compute Terminal Guidance Maneuvers (TGMs). TGM targeting is based on the latest estimate of spacecraft state from the Kalman filter, which encapsulates both navigation and maneuver execution errors. Four TGMs are performed after optical acquisition to correction for navigation and execution errors. TGMs 1 through 3 are targeted using full three-dimensional differential correction while TGM 4 is targeted using two-dimensional B-plane targeting. This was found to be the most robust targeting scheme after initial experimentation because the range between the HAIV and the NEO is not very observable and that compromises targeting schemes that rely solely on full three-dimensional position targeting. The ground-to-ANS handoff occurs at I - 2 hours, at which time the flight dynamics system on the ground provides a final state update to the HAIV and hands over translational control to the ANS. The ANS computes and executes TGMs at I - 90 minutes, I - 35 minutes, I - 12 minutes, and I - 1 minute.

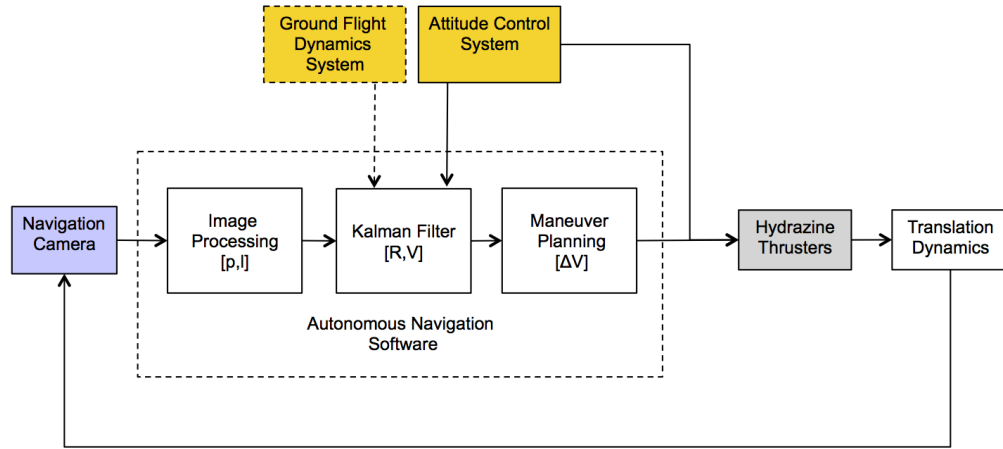
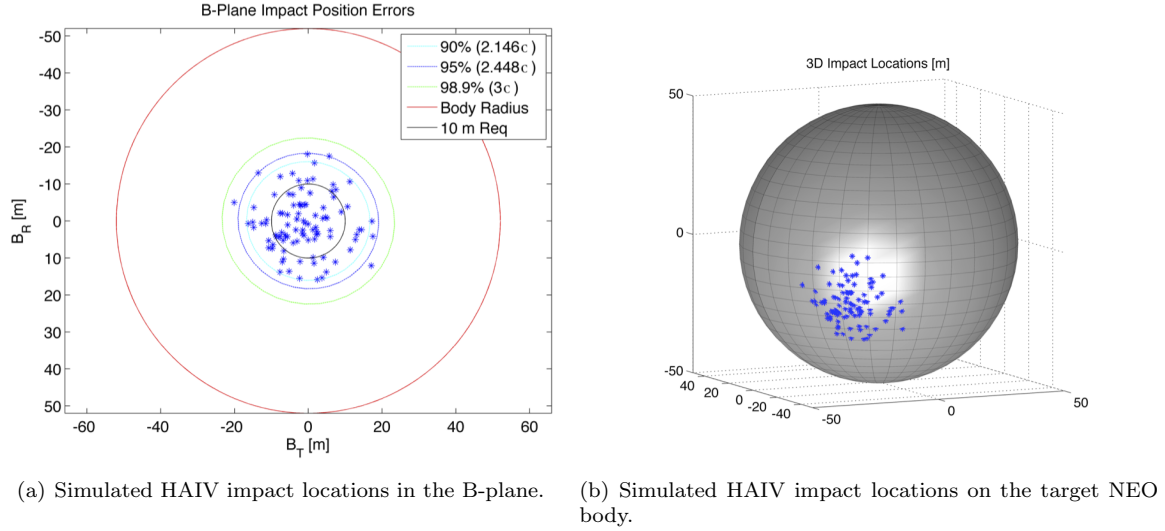


Figure 12. Block diagram of the ANS modeled in simulation.

The ANS was exercised for our target NEO scenario with a Monte Carlo simulation to characterize performance in terms of impact accuracy. Due to study time constraints only 100 Monte Carlo cases were executed to produce the preliminary results shown herein. Figure 13(a) shows the impact locations in the B-plane while Figure 13(b) shows the corresponding impact locations on the body of the target NEO. Note that the area of brightness on the surface of the spherical NEO model shown in Figure 13(b) accurately depicts the solar illumination in the associated mission scenario.

The major axes of the 90%, 95%, and 98.9% impact location error ellipses (which correspond to  $2.146\sigma$ ,  $2.448\sigma$ , and  $3\sigma$  confidences, respectively) are 16.77 m, 19.13 m, and 23.44 m, respectively. Overall, 56% of



**Figure 13. Simulated HAIV impact locations on the target NEO from a Monte Carlo simulation.**

the 100 cases meet the 10 m requirement. While those results do not satisfy the impact accuracy requirement of 10 m with  $3\sigma$  confidence, the impact locations are clearly well-clustered about the center of the NEO and we are working to tune the ANS in ongoing research to meet our accuracy requirement.

A second Monte Carlo analysis using the same simulation parameters described above was performed for a 50 m size NEO to address one of our MDL study goals, which is to assess the feasibility of accurately and reliably intercepting a NEO as small as 50 m at hypervelocity. The impact location errors are shown in Figure 14(a). In this case the major axes of the 90%, 95%, and 98.9% impact location error ellipses are 17.31 m, 19.74 m, and 24.20 m, respectively. Those values are comparable to the values achieved in the 100 m NEO analysis, but the impact location spread relative to the NEO's surface is much larger for the smaller NEO, as seen in Figure 14(a). Another aspect of a 50 m target NEO is that its smaller size will delay optical acquisition compared to the 100 m NEO case, all else being equal. As shown in Figure 14(b), optical acquisition of the 50 m NEO does not occur until I - 18.4 hours for the high albedo case and I - 7.08 hours for the low albedo case. Thus, for a given approach velocity, later acquisitions will require faster ground processing. In some cases it may be possible to re-target the outbound cruise trajectory (from Earth to the NEO) to reduce the approach velocity somewhat, but only to the extent that the crater created by the lead portion of the HAIV still meets mission requirements.

The statistical results for the TGMs for the 100 m NEO analysis are summarized in Table 7. These values informed the construction of the mission  $\Delta v$  budget presented in Table 6.

**Table 7. Terminal Guidance Maneuver (TGM) statistics.**

Maneuver	Minimum (m/s)	Maximum (m/s)	Mean (m/s)	Mean + $3\sigma$ (m/s)
TGM 1 $\Delta v$	0.1557	2.9892	1.1705	3.0643
TGM 2 $\Delta v$	0.0127	0.4065	0.1451	0.3807
TGM 3 $\Delta v$	0.0120	0.5006	0.1812	0.4790
TGM 4 $\Delta v$	0.1689	3.4926	1.3377	3.5045
Total	-	-	2.8345	7.4285

#### VI.D. Attitude Control System

The HAIV Attitude Control System (ACS) is designed to provide stable pointing throughout all mission phases from launch to NEO impact. After launch the ACS will null residual tip-off motion and acquire the



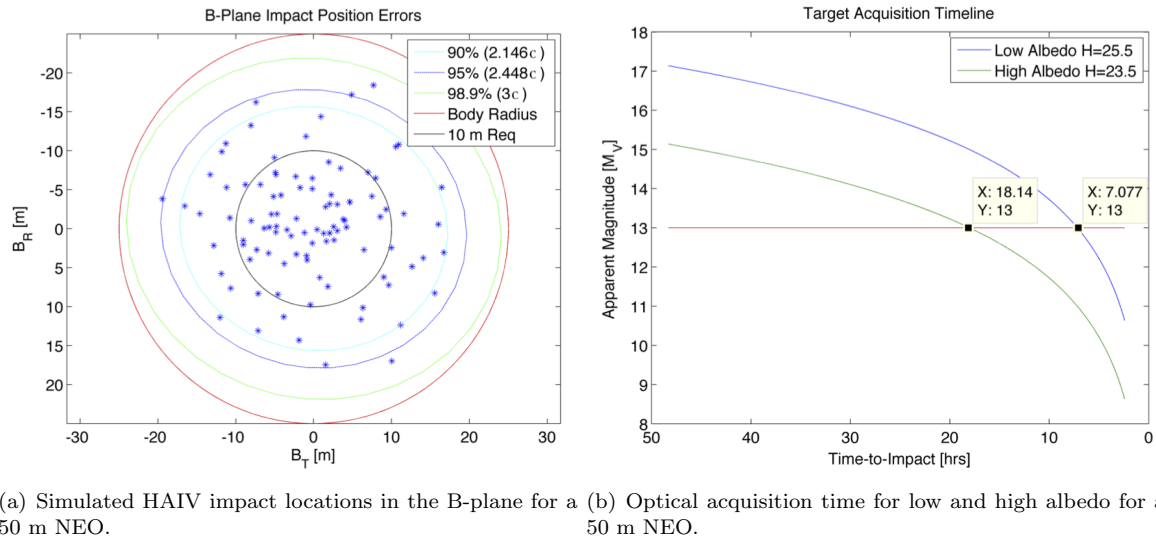


**Figure 14. Timeline for acquisition of a 50 m target NEO and impact accuracy results from a Monte Carlo simulation.**

appropriate mission attitude, with the solar arrays pointing to the Sun. During outbound cruise, up until the terminal approach phase begins, the ACS will facilitate solar array pointing to the Sun (the arrays are able to rotate completely about the  $+Y$  spacecraft body axis). The ACS will also facilitate pointing of the high-gain antenna to the Earth with a pointing accuracy of  $0.1^\circ$ . The antenna can be slewed in two axes over a restricted angular range. The ACS will also keep the cold side of the spacecraft pointed away from the Sun for appropriate thermal control. For maneuvers the ACS will point the thruster centerlines within  $0.5^\circ$  of the designated inertial coordinates. During the terminal approach phase the ACS will nominally hold the  $+X$  spacecraft body axis parallel to the spacecraft's velocity vector. That pointing will be maintained by using thrusters to translate transversely. Additionally, the star camera may be provided as a backup to the impact sensors.

The ACS for this mission requires a relatively straightforward three-axis stabilized system, and the ACS system components are listed in Table 8. The attitude sensors include two star cameras and an inertial reference unit (gyros and possibly an accelerometer package). While two camera heads are baselined in the design, the data processing unit can accommodate up to four camera heads if needed. The attitude actuators include four reaction wheels arranged in a pyramid to provide mutual redundancy along with hydrazine thrusters. The following attitude control modes are defined for this mission: acquisition, cruise,  $\Delta V$ ,  $\Delta H$ , terminal phase, and safehold. The ACS will be operating continuously using the reaction wheels, and the attitude control thrusters will be used at discrete times for momentum unloading. The attitude control thrusters may also be needed during any "turn-and-burn" maneuvers. During the terminal phase, when the ANS is initialized the ACS software will provide the inertial-to-body frame quaternion to the ANS.

**Table 8. Attitude control system components.**

Components	Vendor	Model	Quantity	Total Mass (kg)	Total Avg. Power (W)
IMU	Northrop Grumman	SIRU	1	3.18	20.0
Star Camera	Oersted	Advanced Stellar Compass			
		Camera Heads	2	0.50	1.2
		Data Processing Units	1	0.91	7.0
Coarse Sun Sensors	Adcole	Coarse Solar Sensors	12	0.06	1.2
Reaction Wheels	Honeywell	HR16 (50)	4	48.00	32.0
Total	-	-	-	52.65	58.9

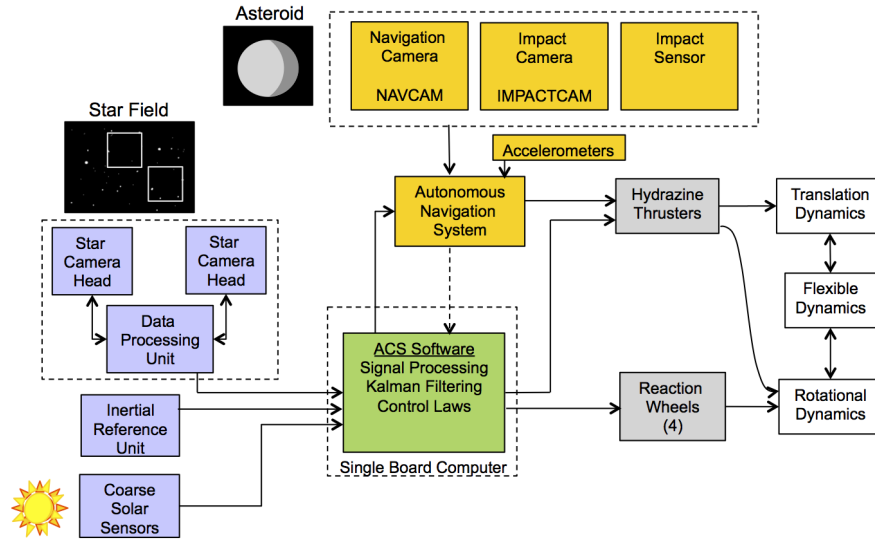


Figure 15. Attitude control system block diagram.

## VI.E. Propulsion

The propulsion system type selected for the HAIV by the MDL is monopropellant hydrazine operating in a blow-down mode from 400 to 100 psi. The system consists of four propellant tanks and twelve 22 N thrusters. The propulsion system is designed to provide  $\Delta v$  and 3-axis attitude control from launch vehicle separation until impact.  $\Delta v$  is available along all the  $+X$ ,  $\pm Y$ , and  $\pm Z$  axes, and the thruster system supports momentum unloading. The propulsion system is designed to be single-fault tolerant. The three-axis attitude control is provided by eight of the thrusters that are canted at  $45^\circ$  and coupled moments are produced by four of the thrusters. The total thrust capability along the  $X$ ,  $Y$ , and  $Z$  directions is 88 N, 31-62 N, and 31-62 N, respectively. For  $\Delta v$  maneuvers in the  $X$  direction there are four thrusters firing continuously with off-pulsing for control. For  $\Delta v$  in the lateral ( $Y$  &  $Z$ ) directions, two thrusters are fired continuously while pulsing two thrusters.

A monopropellant system was selected in favor of a bipropellant system despite the latter's higher efficiency (specific impulse). The rationale for this choice is that the monopropellant diaphragm tanks manage slosh and prevent gas ingestion during lateral burns whereas the bipropellant tanks are susceptible to gas ingestion. Additionally, the monopropellant system is simpler, more reliable, and less expensive, all else being equal.

The thruster ensemble consists of twelve Aerojet MR-106L 22 N thrusters. Each of the four diaphragm tanks is an ATK 80323-1  $23 \times 25$  inch 6Al-4V titanium tab mount tank with a mass of 14.3 kg and a maximum operating pressure of 550 psi. Altogether these four tanks provide a propellant capacity of 360 kg in blow-down mode. All of the components are Commercial Off-The-Shelf (COTS) components. Engineering maneuvers will be performed prior to the terminal phase to characterize thruster performance before terminal maneuvers are executed. The propellant budget is summarized in Table 9 and we note that while the tanks provide a propellant capacity of 360 kg, the current mission design only requires 64 kg of propellant. This provides significant margin for other maneuvering that may be required during the mission due to contingencies. We also note that the burn time for the final TGM is longer than 1 minute, but the final TGM is performed at  $I - 1$  minute. In ongoing work we are therefore trading several design options including increased thrust levels, the timing of the final TGM, and GNC algorithm design strategies that provide sufficient accuracy but purposely keep the final TGM small.

## VI.F. Cost Estimate

The estimated cost of this mission is \$530.4M, including the launch vehicle<sup>1</sup>. The cost estimate is comprehensive and includes the complete design, construction, integration, and testing of the spacecraft itself, launch

<sup>1</sup>An approximate cost of \$150M is assumed for the notional launch vehicle, which is the Atlas V 401

**Table 9. Propellant mass budget.**

Maneuver	$\Delta v$ (m/s)	ACS Tax	Effective $\Delta v$ (m/s)	Effective $I_{sp}$ (s)	HAIV Mass (kg)	Propellant Mass (kg)	Burn Time (s)
Checkout/Engineering Burns	2.3	0	2.30	229	2310.0	2.4	60.4
LV Dispersion, L + 1 day	26.0	50	39.00	229	2307.6	39.8	1014.2
Correction 2, L + 10 days	2.8	50	4.20	229	2267.9	4.2	108.2
Correction 3, L + 30 days	0.3	50	0.45	162	2263.6	0.6	32.1
Correction 4, L + 60 days	0.2	50	0.30	162	2263.0	0.4	21.4
Correction 5, L + 90 days	0.3	50	0.45	162	2262.6	0.6	32.1
TGM 1, I - 90 minutes	3.1	50	4.65	162	2261.9	6.6	330.8
TGM 2, I - 35 minutes	0.4	50	0.60	162	2255.3	0.9	42.6
TGM 3, I - 12 minutes	0.5	50	0.75	162	2254.5	1.1	53.2
TGM 4, I - 1 minutes	3.5	50	5.25	162	2256.4	7.4	372.0
Totals	39.4	-	57.95	-	2246.0 (final)	64.0	2066.8

vehicle integration and test, project management, mission operations, ground system, systems integration and test, education and public outreach, and project reserves.

## VI.G. Key future research topics

Technologies and algorithms must be developed and validated to create sensors capable of accurately and reliably detecting the hypervelocity collision of the impactor with the NEO. These sensors could be hypervelocity electromechanical contact sensors, some form of LIDAR or radar, a visible flash detector, or some other type of device. The number of sensors and the manner of their operation must be such that robust hypervelocity impact detection is provided, i.e., false positives and false negatives must both be prevented with adequate confidence. The appropriate number of sensors will be informed by the type of sensors used, and reliability is a key factor. For example, with 3 sensors providing impact detection signals (to be used as the NED fire command) and the signals being OR'ed, the reliability of each signal would need to be better than 95%. Additional sensors and/or multiple sensor types may be necessary if an adequate confidence of successful fire commanding cannot be provided with a given set of sensors. The design of the hypervelocity impact sensors will be informed by rigorous high-fidelity computational modeling of the hypervelocity kinetic impact event, and ground validation of some candidate sensor types may be possible, e.g., using hypervelocity impact facilities in terrestrial laboratories. Such ground test campaigns could utilize scale models of the HAIV instrumented with candidate impact detection sensors. Another aspect of the design that would benefit tremendously from ground testing is the NED shield. The behavior of the boom during the hypervelocity impact is another key area that must be studied through both high-fidelity computer simulations and possibly ground testing. We must be certain that the size, shape, and materials used to construct the boom fail during the hypervelocity impact in a manner that does not threaten the NED payload, the impact sensors, or the production and reception of the NED fire command signal. This raises the possibility of another trade study that we are considering, the purpose of which is to assess the feasibility, advantages, and disadvantages of having the impactor and follower be physically separated free-flying vehicles rather than connected by a boom.

Another key area of analysis is the final approach timeline. Our results presented herein demonstrate that the final approach timeline depends on the target NEO diameter and albedo, as well as the approach phase angle relative to the NEO and the relative velocity at impact. Developing parametric models for the approach timeline as a function of these and other key driving parameters will facilitate refinement of the onboard optical systems to ensure acquisition of the target sufficiently far in advance of the impact for the ANS to be able to operate robustly and achieve a precise and accurate impact with high confidence. We can also adjust our trajectory optimization algorithms to attempt to minimize the intercept velocity within the constraints that the crater excavated on the NEO is of sufficient depth and that the additional maneuver required for intercept velocity control is within our available  $\Delta v$  budget.

Finally, the results presented herein clearly demonstrate that further work is required to improve the

performance and robustness of the ANS, particularly in terms of the terminal GNC algorithms. The accuracy must be improved so that statistical impact locations on the NEO surface are always tightly clustered about the NEO center, and the algorithms must be structured to minimize the magnitude of the last TGM or two such that achieving them is well within the capability of the propulsion system (e.g., the accelerations requested by the GNC system are readily achievable given the spacecraft mass and available thrust). The GNC algorithms will also be upgraded to process synthetic imagery for realistic cases including irregularly shaped rotating NEOs of various sizes to demonstrate that the GNC system is robust to a wide variance in NEO properties. This robustness is important because we will generally not have much information on the physical properties of the NEO before the HAIV is deployed during an actual mission scenario. Accordingly, we are also assessing the effects of NEO density (which will not generally be known in advance) on the cratering performance of the kinetic impactor portion of the HAIV in order to ensure sufficient crater depth for the NED detonation.

## VII. Conclusions

Earth has been struck by asteroids and comets in the past and will continue to be struck now and in the future. Our geological records, historical records, observations of recent events, and foreknowledge of upcoming events provide us with ample evidence that the threat of Earth impact by hazardous NEOs is quite real. Although we have sent a number of scientific missions to NEOs, we have never before performed actual flight demonstrations of the planetary defense technologies that we will need to rely upon during a true emergency situation. The goal of our Phase 2 NIAC research project is to design a feasible, effective, and reliable HAIV for planetary defense and also design a flight validation mission during which its effectiveness and reliability will be demonstrated. The HAIV is a two-body spacecraft consisting of a lead kinetic impactor portion that excavates a shallow crater on the target NEO into which the follower portion of the spacecraft delivers a NED and detonates it to perform a subsurface detonation that is approximately 20 times more effective at disrupting the NEO than a surface or standoff detonation. The ability to carry out that sequence at intercept velocities in the hypervelocity regime (5–30 km/s), combined with the high efficiency of subsurface detonations, makes the HAIV a highly responsive planetary defense platform for a wide range of hazardous NEO scenarios. In particular, the HAIV provides a viable planetary defense solution for short warning scenarios involving small but dangerous NEOs in the 50 to 100 m size category or larger.

In this paper we have provided background on the threat NEOs pose to Earth, an overview of the NEO missions that have been performed to date and why they do not constitute planetary defense technology demonstrations, a description of the HAIV concept, and the results of a recent NASA/GSFC MDL study for the conceptual design of the HAIV flight validation mission in collaboration with the ADRC of Iowa State University as part of the Phase 2 NIAC project research.

The MDL study has provided a feasible and detailed conceptual design for the HAIV flight validation mission and identified a number of key topics for further research that are being pursued by the ADRC and GSFC as part of the ongoing Phase 2 NIAC work. These research topics include high-fidelity computational modeling of hypervelocity impact physics, detailed development of advanced GNC algorithms for precision hypervelocity intercept of small (50–100 m size) NEOs, and design and development of test plans for robust hypervelocity impact sensors. In our ongoing research we will continue to refine, deepen, expand, and advance the design of the HAIV system and its flight validation mission.

When a hazardous NEO on a collision course with Earth is discovered we will not have the luxury of designing, testing, and refining our systems and plans. We will need to be prepared to take effective action on relatively short notice with a high probability of succeeding on the first try because we may not have a second chance. That level of adeptness and preparedness can only be achieved through proper design and testing of systems now so that we are comfortable with carrying out planetary defense test and practice missions before we need to deploy such a mission in response to an actual threat.

## Acknowledgments

This research has been supported by a NIAC (NASA Innovative Advanced Concepts) Phase 2 study grant. The authors would like to thank Dr. John (Jay) Falker, the NIAC Program Executive, for his support.

## References

- <sup>1</sup>Wie, B., Pitz, A., Kaplinger, B., Hawkins, M., Wagner, S., Vardaxis, G., Winkler, T., and Lyzhoft, J., “Optimal Fragmentation and Dispersion of Hazardous Near-Earth Objects,” NIAC Phase I Final Report, Grant Number NNX11AR43G, Asteroid Deflection Research Center, Department of Aerospace Engineering, Iowa State University, Ames, IA, September 2012.
- <sup>2</sup>Vardaxis, G., Pitz, A., and Wie, B., “Conceptual Design and Analysis of Planetary Defense Technology (PDT) Demonstration Missions,” *Advances in the Astronautical Sciences*, Vol. 143, Univelt, Inc., San Diego, CA, 2012, Paper number AAS 12-128.
- <sup>3</sup>Pitz, A., Kaplinger, B., Vardaxis, G., Winkler, T., and Wie, B., “Conceptual Design of a Hypervelocity Asteroid Intercept Vehicle (HAIV) and Its Flight Validation Mission,” *Proceedings of the 2012 IAF/AIAA Global Space Exploration Conference*, Washington, DC, May 22-24, 2012. Paper number GLEX-2012.06.312173.
- <sup>4</sup>Winkler, T., Wagner, S., and Wie, B., “Optimal Target Selection for a Planetary Defense Technology (PDT) Demonstration Mission,” *Advances in the Astronautical Sciences*, Vol. 143, Univelt, Inc., San Diego, CA, 2012, Paper number AAS 12-226.
- <sup>5</sup>Wagner, S., Winkler, T., and Wie, B., “Analysis and Selection of Optimal Targets for a Planetary Defense Technology Demonstration Mission,” *Proceedings of the 2012 AIAA/AAS Astrodynamics Specialist Conference*, Minneapolis, MN, August 13-16, 2012. AIAA Paper Number 2012-4874.
- <sup>6</sup>Wagner, S., Wie, B., Barbee, B. W., “Target Selection for a Hypervelocity Asteroid Intercept Vehicle Flight Validation Mission,” *Proceedings of the IAA Planetary Defense Conference 2013*, Flagstaff, AZ, April 15-19, 2013.
- <sup>7</sup>Barbee, B.W., Abell, P.A., Adamo, D. R., Alberding, C. M., Mazanek, D. D., Johnson, L. N., Yeomans, D. K., Chodas, P. W., Chamberlin, A. B., Friedensen, V. P., “The Near-Earth Object Human Space Flight Accessible Targets Study: An Ongoing Effort to Identify Near-Earth Asteroid Destinations for Human Explorers,” *Proceedings of the IAA Planetary Defense Conference 2013*, Flagstaff, AZ, April 15-19, 2013.